Progress In Electromagnetics Research, Vol. 105, 333–346, 2010

GENERALIZED EQUIVALENT CONDUCTOR METHOD FOR A CHAFF CLOUD WITH AN ARBITRARY ORIENTATION DISTRIBUTION

D.-W. Seo

Department of Electrical Engineering
KAIST
335 Gwahangno, Yuseong-gu, Daejeon 305-701, Korea

J.-H. Yoo and K. I. Kwon

Agency for Defense Development
P. O. Box 35-3, Yuseong, Daejeon 305-600, Korea

N.-H. Myung

Department of Electrical Engineering
KAIST
335 Gwahangno, Yuseong-gu, Daejeon 305-701, Korea

Abstract—A recently presented equivalent conductor (EC) method enables fast computation for the radar cross section (RCS) of a chaff cloud. Despite its good performance, the EC method is restrictively applicable due to the complex orientation distribution of chaff and the incident angle. In this paper, a generalized equivalent conductor (GEC) method is presented for estimating the RCS of an actual chaff cloud. The proposed method can be applied to any orientation distribution of the chaff cloud by using a weight function and a weighted average, as well as to any incident angle by employing a method of moment (MoM). Numerical results are presented for three scenarios and validated with results of the MoM.

Corresponding author: D.-W. Seo (SeoDongwook@kaist.ac.kr).

1. INTRODUCTION

Chaff is one of the simplest radar countermeasures. Chaff consists of a bunch of small, thin metalized glass fibers or wire and is spreaded through the chaff cartridge on aircrafts or warships. Dispersed chaff fibers fall in the air in the shape of a cloud. The reflected signal from the chaff cloud disturbs the opponent's radar system. Since chaff is relatively cheap and efficient, it is used in most military aircrafts and warships for self-defense. Accordingly, study of the characteristics of electromagnetic scattering by the chaff cloud is important for ensuring survival in electronic warfare.

Mutual coupling is the most important problem in calculating the scattering of multiple scatterers. In particular, when scatterers are densely placed, mutual coupling between scatterers is strong and a tremendous amount of calculations is required to take this phenomenon into account. The difficulty of estimating the radar cross section (RCS) of a chaff cloud arises from the huge dimension of the analysis region and extremely large number of scatterers. The number of chaff fibers is generally in the range of several millions. Therefore, the analysis of electromagnetic scattering by the chaff cloud imposes an enormous calculation burden, thus making it impractical for real application. For these reasons, in most cases, the RCSs of the chaff cloud are simply expressed as the product of the total number of chaff fibers and average RCS of a single chaff fiber [1, 2]. However, this method is only valid when the distance between neighboring fibers is larger than 2λ so the effect of mutual coupling can be ignored. Thus, if mutual coupling is not considered, coarse results can be obtained when scatterers are densely placed.

Several methods have been developed to analyze multiple scattering by multiple wire scatterers [3–10]. Among these methods, the equivalent conductor (EC) method recently proposed in [7] considers the chaff cloud as a homogeneous medium with effective permittivity that depends on the average density, the length of chaff fibers, and operating frequency. The coherent and incoherent RCS of the chaff cloud can then be calculated quickly and easily from the homogeneous medium [7, 8]. Therefore, at present, the EC method is the most powerful approach for analyzing the chaff cloud. Unfortunately, this approach has some drawbacks. First, it can only be used when all scatterers are oriented to the same probability in all directions. Since general chaff fibers have a high aspect ratio, that is, the ratio of the length to the diameter of the scatterer, chaff fibers maintain a horizontal orientation in the air for 1–2 hours [11, 12]. Therefore, the EC method cannot be used to calculate the RCS of the

actual chaff cloud, because the actual chaff does not have a random orientation in all directions. Second, the monostatic RCS can only be found by a scattering plane-based system with an incident zenith angle of 90° (elevation angle of 0°) to the chaff cloud. However, most radar systems are ground-based in practice. Situations with an incident zenith angle of 90° are rare except when the chaff fibers are sprinkled into the air to deceive aircrafts. In this paper, we propose a generalized EC (GEC) method to overcome the drawbacks of the EC method.

2. BRIEF REVIEW OF THE EQUIVALENT CONDUCTOR (EC) METHOD [7]

Wires are randomly distributed through a rectangular cuboid shaped slab in Fig. 1(b) and oriented with the same probability in all directions. When a plane wave is normally incident on the slab, the effective permittivity of the slab is given by

$$\varepsilon_{eff} = \varepsilon' - j\varepsilon'' = \varepsilon_0 \left(1 - j\frac{\eta_0}{2\pi} \cdot \rho\lambda^3 \cdot \frac{l}{\lambda} \cdot \bar{\mathbf{I}}\right), \tag{1}$$

where η_0, ρ, l, and λ denote the intrinsic impedance of free space, the average density of wires (the number of wires per cubic lambda), the length of wires, and the wavelength in free space, respectively. $\bar{\mathbf{I}}$ is an

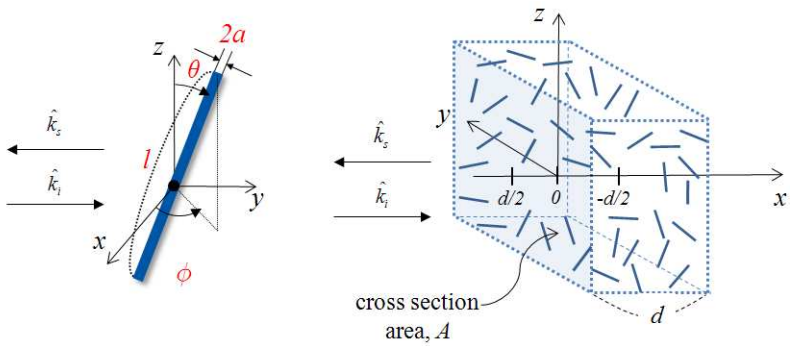

Figure 1. (a) Coordinate system for a single fiber. (b) Geometry of a slab with width d, cross section area A and volume V for the chaff cloud.

effective average current and is given by

$$\bar{\mathbf{I}} = \frac{1}{4\pi} \int_0^{\pi} d\theta \sin\theta \int_0^{2\pi} d\phi \tilde{\mathbf{I}}(\theta, \phi), \tag{2}$$

where $\tilde{\mathbf{I}}(\theta, \phi)$ is an actual current component. As shown in Fig. 1(a), θ and ϕ are the zenith and azimuth angles of the fiber orientation, respectively. In (2), the effective average current $\bar{\mathbf{I}}$ denotes the average value of the actual current component $\tilde{\mathbf{I}}(\theta, \phi)$ for all directions.

In the EC method, the actual current component $\tilde{\mathbf{I}}(\theta, \phi)$ is given by

$$\tilde{\mathbf{I}}(\theta, \phi) = \hat{l}(\theta, \phi) \int_{-l/2}^{l/2} I\left(l'; \theta, \phi\right) e^{jk_0 l' \cos\theta} dl', \tag{3}$$

where $\hat{l}(\theta, \phi)$ is the direction vector of the fiber. The actual current component $\tilde{\mathbf{I}}(\theta, \phi)$ is the integration of the equivalent line source and denotes the current component inducing the scattered wave in a $\hat{k}_s = -\hat{x}$ direction from a single wire having a direction of $\hat{l}(\theta, \phi)$.

3. GENERALIZED EQUIVALENT CONDUCTOR (GEC) METHOD

3.1. Consideration of Incident Angle and Polarization

Unfortunately, Equation (3) only contains information about the scattered angle ($\hat{k}_s = -\hat{x}$), and does not provide further information about the incident angle, incident polarization, or scattered polarization. From (3), it is not possible to directly obtain the actual current component inducing the scattered wave with a certain scattered angle and polarization when a single wire is illuminated by a certain incident wave with an arbitrary polarization and incident angle. Thus, additional complex procedures are needed to derive the actual current component $\tilde{\mathbf{I}}(\theta, \phi)$.

If the orientation of scatterers is uniformly random for all directions, the chaff cloud is an isotropic medium; in this case, neither the incident angle and polarization nor the scattered angle and polarization are important issues. However, if the chaff cloud is an anisotropic medium, the RCS of the chaff cloud will vary extensively depending on the angle and polarization.

In order to calculate the actual current component $\tilde{\mathbf{I}}(\theta, \phi)$, including information about the incident and scattered wave, we

redefine the actual current component $\tilde{\mathbf{I}}(\theta,\phi)$ using a method of moment (MoM) as follows:

$$\tilde{\mathbf{I}}_{pq}(\theta,\phi;\theta_s,\phi_s;\theta_i,\phi_i) = \mathbf{R}_p^T \mathbf{Z}^{-1} \mathbf{V}_q \tag{4}$$

where p and q can be either θ or ϕ (p, $q = \theta$, ϕ). The first subscript specifies the polarization of the scattered wave and the second the polarization of the incident wave. $\mathbf{Z}$ is the impedance matrix of a single wire and T is the transpose operator. $\mathbf{R}$ and $\mathbf{V}$ are the measurement vector and excitation vector, respectively. The exact expressions of the elements of $\mathbf{R}$ and $\mathbf{V}$ are as follows [13]

$$V_m^{p(\text{or } q)}(\theta_i,\phi_i) = \iint_{S_m} \vec{W}_m(\vec{r}) \cdot \hat{p}\,(\text{or } \hat{q})\, e^{-jk_0 \hat{k}_i \cdot \vec{r}} ds \tag{5}$$

$$R_n^{p(\text{or } q)}(\theta_s,\phi_s) = \iint_{S_n} \vec{J}_n(\vec{r}') \cdot \hat{p}\,(\text{or } \hat{q})\, e^{-jk_0 \hat{k}_s \cdot \vec{r}} ds' \tag{6}$$

where $\vec{W}_m$ and $\vec{J}_n$ are the testing function and basis function, respectively. The incident and scattered wave vectors are

$$-\hat{k}_i = \hat{x}\sin\theta_i\cos\phi_i + \hat{y}\sin\theta_i\sin\phi_i + \hat{z}\cos\theta_i, \tag{7}$$

$$\hat{k}_s = \hat{x}\sin\theta_s\cos\phi_s + \hat{y}\sin\theta_s\sin\phi_s + \hat{z}\cos\theta_s. \tag{8}$$

Information about the incident angle and polarizations is included in (5) and (7), and information about the scattered angle and polarizations is included in (6) and (8).

From (5) through (8), the incident and scattered angles can have different and arbitrary angles. However, because the homogeneous medium is in the form of a slab, there is no meaning other than backscattering and forward scattering. Nevertheless, it is important that the incident and scattered angle (θ_i, θ_s) can be set to an arbitrary angle. By rotating the slab, as shown in Fig. 2, the wave is normally incident on the slab but obliquely incident on the individual fibers.

For a monostatic RCS ($\theta_i = \theta_s$ and $\phi_i = \phi_s$), the actual current component $\tilde{\mathbf{I}}_{pq}(\theta,\phi;\theta_i,\phi_i)$ can be calculated in the form of 2 by 2 matrices for every polarization transverse to the propagation direction.

$$\tilde{\mathbf{I}}(\theta,\phi;\theta_i,\phi_i) = \begin{bmatrix} \tilde{\mathbf{I}}_{\theta\theta}(\theta,\phi;\theta_i,\phi_i) & \tilde{\mathbf{I}}_{\theta\phi}(\theta,\phi;\theta_i,\phi_i) \\ \tilde{\mathbf{I}}_{\phi\theta}(\theta,\phi;\theta_i,\phi_i) & \tilde{\mathbf{I}}_{\phi\phi}(\theta,\phi;\theta_i,\phi_i) \end{bmatrix} \tag{9}$$

3.2. Consideration of Arbitrary Orientation Distribution

The effective average current $\bar{\mathbf{I}}$ in (3) is the average value of the actual current component $\tilde{\mathbf{I}}(\theta,\phi)$. In the EC method, it is calculated by the unweighted average of (2), and thus this approach is only applicable to

randomly oriented wires. If the orientation of scatterers is uniformly random for all directions, the result induced by only one polarization is needed, since $\bar{\mathbf{I}}_{\theta\theta} = \bar{\mathbf{I}}_{\phi\phi}$ and $\bar{\mathbf{I}}_{\theta\phi} = \bar{\mathbf{I}}_{\phi\theta} = 0$. However, $\bar{\mathbf{I}}_{\theta\theta}$ and $\bar{\mathbf{I}}_{\phi\phi}$ are no longer the same if the orientation of wires is not uniformly random for all directions.

In order to consider an arbitrary orientation distribution of wires, we propose that the effective average current be calculated by weighting for the majority distributed orientation more than others. The unweighted average of (2) can then be converted to the weighted average as follows:

$$\bar{\mathbf{I}}_{pq}(\theta_i, \phi_i) = \frac{\int\limits_{\Omega} \tilde{\mathbf{I}}_{pq}(\theta, \phi; \theta_i, \phi_i)\, W(\theta, \phi)\, d\theta d\phi}{\int\limits_{\Omega} W(\theta, \phi)\, d\theta d\phi}, \tag{10}$$

where $W(\theta, \phi)$ is the weight function in the form of a probability density function (pdf) which represents the orientation distribution of wires in air. Once $\tilde{\mathbf{I}}_{pq}(\theta, \phi; \theta_i, \phi_i)$ is calculated, the effective average current $\bar{\mathbf{I}}_{pq}(\theta_i, \phi_i)$ considering the orientation distribution of wires can be obtained by using the weighted average of (10).

The permittivity takes different values in different directions, because scatterers are oriented with different probability in different directions. Hence, the chaff cloud is an electrically anisotropic medium and must be described by a dyadic effective permittivity:

$$\bar{\bar{\varepsilon}}_{eff} = \hat{\theta}\hat{\theta}\varepsilon_{\theta\theta} + \hat{\theta}\hat{\phi}\varepsilon_{\theta\phi} + \hat{\phi}\hat{\theta}\varepsilon_{\phi\theta} + \hat{\phi}\hat{\phi}\varepsilon_{\phi\phi}, \tag{11}$$

where ε_{pq} is calculated by the effective average current having a component in the direction of p-polarization and an incident wave with

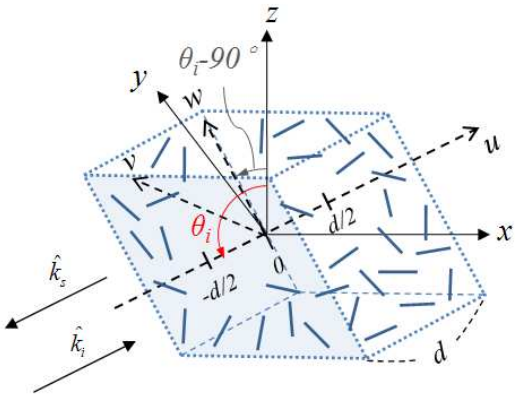

Figure 2. Geometry of tilted slab for normal incidence.

q-polarization as follows:

$$\varepsilon_{pq} = \varepsilon_0 \left(1 - j\frac{\eta_0}{2\pi} \cdot \rho\lambda^3 \cdot \frac{l}{\lambda} \cdot \bar{\mathbf{I}}_{pq}\right) = \varepsilon_0 \left(1 - js_{pq}\right). \tag{12}$$

If M_1 wires of length l_1 and M_2 wires of length l_2 are uniformly distributed within a volume V, then ε_{pq}, by employing the basic principles of the EC method, is written as

$$\varepsilon_{pq} = \varepsilon_0 \left[1 - j\frac{\eta_0}{2\pi} \cdot \left(\frac{M_1}{V}\lambda^3 \cdot \frac{l_1}{\lambda} \cdot \bar{\mathbf{I}}_{1,pq} + \frac{M_2}{V}\lambda^3 \cdot \frac{l_2}{\lambda} \cdot \bar{\mathbf{I}}_{2,pq}\right)\right], \tag{13}$$

where the effective average current $\bar{\mathbf{I}}_{1,pq}$ by the wires of length l_1 depends on the length and orientation distribution of wires, the frequency, incident angle, scattered angle, and polarization.

A quantity of chaff fibers dispersing in the air can be replaced by a homogeneous medium having effective permittivity, $\bar{\bar{\varepsilon}}_{eff}$. From the homogeneous medium, the coherent RCS σ_{coh} is calculated by (37) of [7] based on the boundary value solution and the incoherent RCS σ_{incoh} is calculated by (19) of [8]. The total RCS is the sum of the coherent and incoherent RCS, given as follows:

$$\sigma = \sigma_{coh} + \sigma_{incoh}. \tag{14}$$

4. NUMERICAL RESULTS

Depending on the ratio of parallel chaff to the horizontal plane (xy-plane) to the total chaff in number, the orientation distribution can be classified into three cases.

For the first case, assume that the chaff fibers have a uniformly random orientation for all directions. The weight function in the pdf form is given as follows:

$$W(\theta) = \frac{1}{2}\sin\theta, \quad W(\phi) = \frac{1}{2\pi}. \tag{15}$$

In the second case, the number of chaff fibers oriented parallel to the xy-plane is larger than that of the first case. Since it cannot be concisely described in pdf form, the weight function is represented by a Gaussian distribution with a mean of 90° and a standard deviation of 20°.

$$W(\theta) = \frac{1}{\sqrt{2\pi\sigma^2}} e^{-(\theta-\mu)^2/2\sigma^2}, \quad W(\phi) = \frac{1}{2\pi}. \tag{16}$$

Finally, if all chaff fibers are oriented horizontally, then the weight function is

$$W(\theta) = \delta\left(\theta - \frac{\pi}{2}\right), \quad W(\phi) = \frac{1}{2\pi}. \tag{17}$$

Table 1. The mean and standard deviation of the zenith angle of chaff fibers for Case 1, Case 2, and Case 3.

	Mean (deg.)	*Standard deviation* (deg.)
Case 1	90°	39°
Case 2	90°	20°
Case 3	90°	0°

For all three cases, the zenith orientation angles of the chaff fibers have different distributions. The mean and standard deviation of the zenith orientation angles in the three cases are summarized in Table 1. Case 1 has a high standard deviation. That is, the zenith orientation angles of the chaff fibers are spread over a larger range than in the other cases, whereas the standard deviation of case 3 has 0°. Therefore, all the chaff fibers of case 3 have a zenith angle of exactly 90°.

Each wire scatterer is thin, has a half-wavelength, and is perfectly-conducting and uniformly distributed throughout the slab. The cross-sectional area of the slab is fixed as $A = 10\lambda \times 10\lambda$, while the depth of the slab d varies from 0.1λ to 4λ. The density of wires ρ is set to 1.0 [No./λ^3]. Fig. 3 displays the backscattering RCS of the chaff cloud normalized to λ_0^2, in resonance frequency as a function of the depth of the slab, when the chaff cloud is illuminated by a plane wave incident at $\theta_i = 135°$. In order to verify the result obtained by the proposed method, as a reference solution we perform a Monte Carlo simulation using the MoM with 50 realizations, employing MATLAB 7.0 with a 2.83 GHz Quad CPU and a 8 Gbyte RAM PC.

For the first case, as shown in Fig. 3, $\sigma_{\phi\phi}$ and $\sigma_{\theta\theta}$ are almost the same and appear to overlap, since all the chaff fibers are oriented with the same probability in all directions. As the orientation of the wires becomes parallel to the horizontal plane, $\sigma_{\phi\phi}$ increases while $\sigma_{\theta\theta}$ decreases. Thus, the difference between $\sigma_{\phi\phi}$ and $\sigma_{\theta\theta}$ becomes larger. Cases 2 and 3 show roughly a 1.5 dB and 6 dB difference between $\sigma_{\phi\phi}$ and $\sigma_{\theta\theta}$, respectively. For the three orientation distributions, the results obtained by the proposed method are in good agreement with those obtained by the MoM.

In the GEC method, the greatest portion of time is devoted to calculation of the effective average current. If the effective average current is known, the RCS can be easily obtained by substituting the effective average current $\bar{\mathbf{I}}_{pq}(\theta_i, \phi_i)$ into the given equations. In case 3, the CPU time for computing the RCS versus the depth of the slab consumed using the proposed method and the MoM were 0.03 sec and 15 hours, respectively. Clearly, the proposed method showed massive

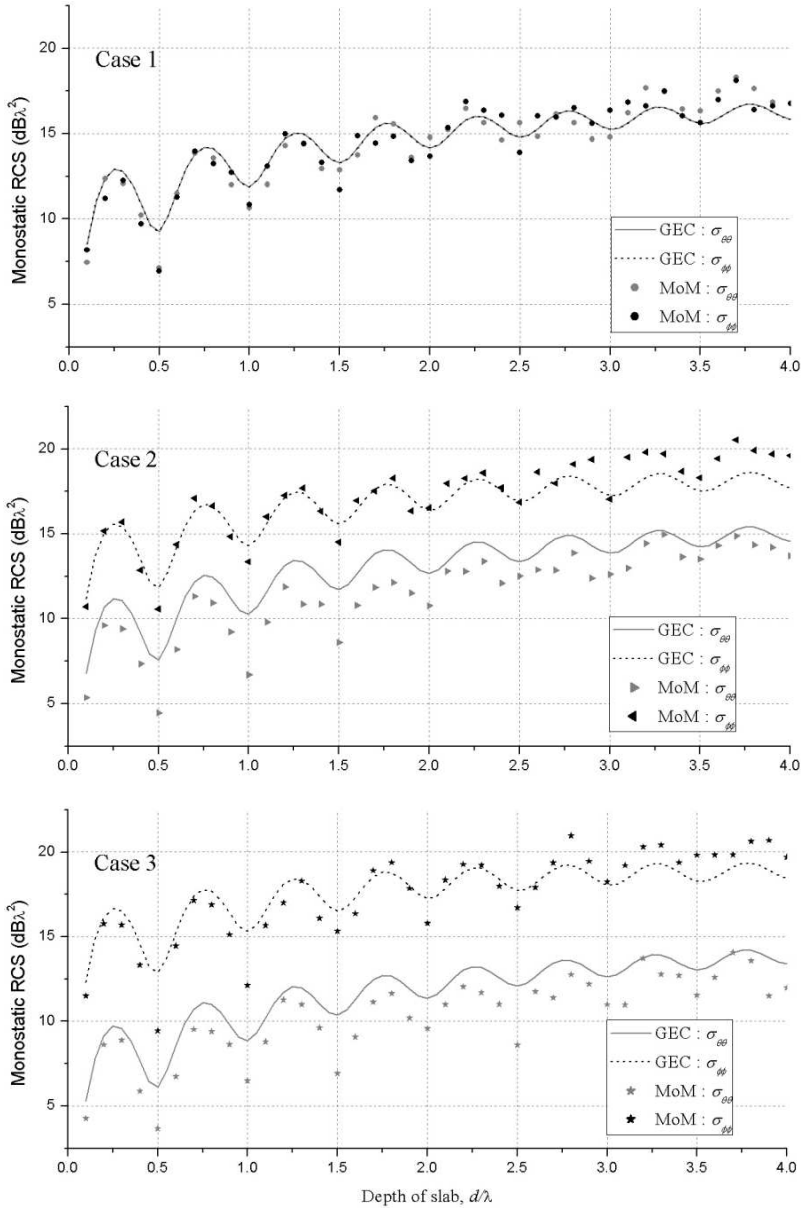

Figure 3. Normalized monostatic RCS of chaff cloud with orientation distribution of case 1, case 2 and case 3 at an incident zenith angle of 135°.

improvement in computing speed over the MoM approach.

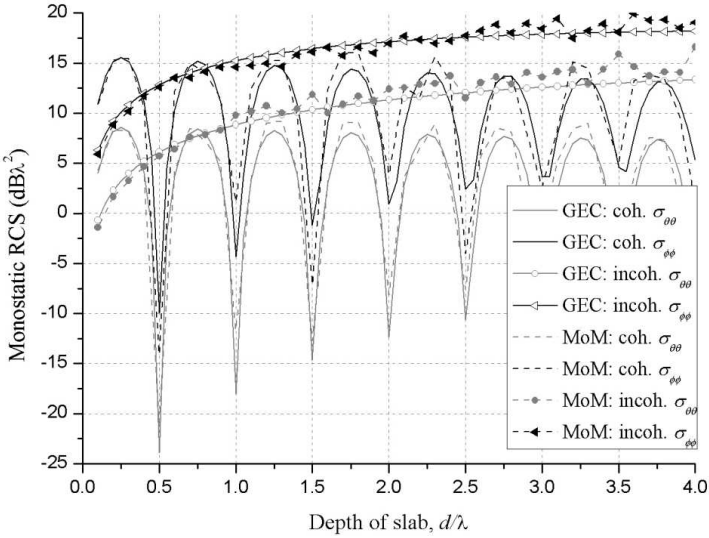

Figure 4. Normalized coherent and incoherent backscattering RCS of case 3.

The average RCS of the random media can be expressed as the sum of the coherent RCS and the incoherent RCS [7, 14]. The RCS of the homogeneous medium is also obtained as the sum of the coherent RCS and the incoherent RCS. Fig. 4 shows the backscattering RCS of case 3, expressed as the coherent RCS and the incoherent RCS. The graph of the coherent RCS has null points at the depth of the slab, $d/\lambda = n/2$, where n is the positive integer. The coherent RCS oscillates with peaks of a constant level. On the other hand, the incoherent RCS has a small value in the case of a small number of scatterers and its value increases as the number of scatterers increases. Note that it has larger values than the coherent RCS when d is greater than or equal to 0.8λ. Therefore, the total RCS of the random media expressed as the sum of the coherent RCS and incoherent RCS retains oscillation with an increase in the overall level as the depth of the slab increases for all cases, as shown in Fig. 3.

Figure 5 shows the RCS of the chaff cloud under the same condition as case 3 when a plane wave is incident on the chaff cloud at $\theta_i = 90°$. $\sigma_{\phi\phi}$ of $\theta_i = 90°$ has a similar level when $\theta_i = 135°$, but $\sigma_{\theta\theta}$ of $\theta_i = 90°$ has a very small value. For the incident wave with $\theta_i = 90°$, θ-polarization is the same as z-polarization according to the coordinate transformation. Since all chaff fibers of case 3 are

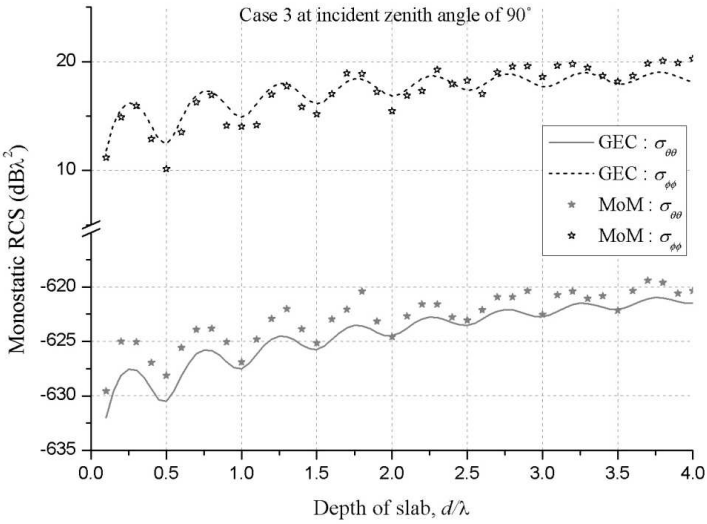

Figure 5. Normalized monostatic RCS of chaff cloud with orientation distribution of case 3 at an incident zenith angle of 90°.

horizontally oriented, there is no component in the z-direction. Thus, $\sigma_{\theta\theta}$ should be identically zero for the case of $\theta_i = 90°$. The results of $\sigma_{\theta\theta}$, however, give a value of about $-625\,\mathrm{dB}\lambda^2$, due to the numerical precision of the computer. On the other hand, since the unit vector of the θ-direction is $\hat{\theta} = \hat{x}\frac{\cos\phi_i}{\sqrt{2}} + \hat{y}\frac{\sin\phi_i}{\sqrt{2}} - \hat{z}\frac{1}{\sqrt{2}}$ for a plane wave with $\theta_i = 135°$, the θ-polarized plane wave is affected by the x, y, and z-components of the wires, and thus $\sigma_{\theta\theta}$ has about a 5–12 $\mathrm{dB}\lambda^2$ level at this incident angle. These results imply that the RCS of the chaff cloud is greatly affected by only a slight change of the incident angle. For the RCS calculation of the chaff cloud, therefore, the incident angle should be taken into careful consideration, since the scatterers to be aligned along one direction as time passes are significantly affected by this variable.

Because of the assumption that all chaff fibers have identical length, the RCS of the chaff fibers is calculated in resonance frequency. If more than two types of wires are used as the chaff, the frequency response of the chaff fibers is needed. Consider five hundred wires of length l_1 and five hundred wires of length l_2 $(= 0.896l_1)$ uniformly distributed in a cube of $1.0\,\mathrm{m}^3$. The orientation of the chaff fibers is uniformly random for all directions. Fig. 6 shows the $\theta-\theta$ polarization RCS of the chaff fibers as a function of frequency when a plane wave illuminates with $\theta_i = 90°$. To verify the results of the GEC method, the

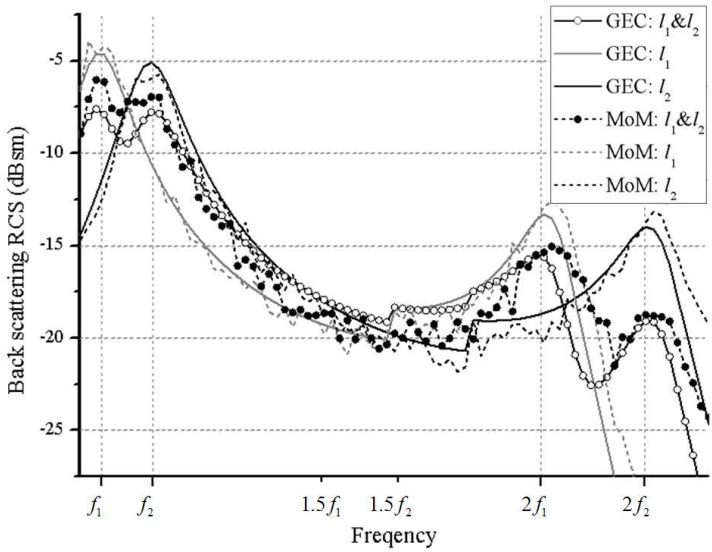

Figure 6. Monostatic RCS of chaff cloud (cube of $1.0\,\mathrm{m}^3$) with two types of wires at an incident zenith angle of 90°: comparison of results obtained by the GEC with the MoM. (f_1: the first resonance frequency of a wire of length l_1, f_2: the first resonance frequency of a wire of length l_2, and $l_1 = 1.116l_2$).

results of the MoM are calculated by averaging the RCSs at intervals of 10° in a range of $\phi_i = 0$–360°. For comparison with the frequency responses by only one type of wires and two types of wires, we calculate the RCSs of one thousand wires of length l_1 and length l_2, respectively.

The solid line of the GEC method and the dashed line of the MoM show a similar pattern. However, the results of the MoM do not fall on a smooth line. The main reason for this is that the number of samples obtained by the MoM is not sufficient in the averaging process. In the case of using one type of wire, peaks appear at the first and second resonance frequencies. For coexistence of the wires of length l_1 and length l_2, the backscattering RCS has peaks at the resonance frequencies of the wires of length l_1 as well as length l_2 and approximately corresponds with the average of the RCSs of one thousand wires of length l_1 and length l_2.

5. CONCLUSION

A generalized EC (GEC) method for calculating the RCS of a chaff cloud has been introduced in this paper. The RCS by an arbitrary incident angle and polarization can be calculated by finding the actual current component via the MoM. Moreover, the RCS of a chaff cloud having an arbitrary orientation distribution can be found by calculating the effective average current based on a weight function which represents the orientation distribution of the chaff fibers. Unlike general numerical methods such as the MoM and Finite-Difference Time-Domain (FDTD), the GEC method does not require the exact location or orientation of the chaff fibers; only the density and the orientation distribution (mean and standard deviation) of the chaff fibers are needed. In addition, multiple scatterers are considered as a homogeneous medium, and the RCS is then calculated from this homogeneous medium. Therefore, fast computation becomes possible for the RCS calculation of the chaff cloud. The proposed GEC method is verified through comparison with a backscattered RCS calculation using the MoM. We demonstrate that the GEC method achieves good accuracy with a very low computation burden.

If the chaff cloud is divided into multiple sub-blocks, and the total RCS is calculated by the sum of the RCS of all sub-blocks by the proposed method, the RCS of a chaff cloud with several million fibers can be obtained.

ACKNOWLEDGMENT

This research was supported by the Agency for Defense Development, Korea, through the Radiowave Detection Research Center at KAIST.

REFERENCES

1. Macedo, A. D. F., "Analysis of chaff cloud RCS applying Fuzzy Calculus," *Proc. 1997 SBMO/IEEE MTT-S Int. Microwave and Optoelectronics Conf.*, Vol. 2, 724–728, Brazil, Aug. 1997.
2. Pouliguen, P., O. Bechu, and J. L. Pinchot, "Simulation of chaff cloud radar cross section," *Conf. 2005 IEEE Antennas Propag. Society Int. Symp.*, Vol. 3A, 80–83, Wasington DC, USA, Jul. 2005.
3. Nagl, A., D. Ashrafi, and H. Uberall, "Radar cross section of thin wires," *IEEE Transaction on Antennas and Propagation*, Vol. 39, No. 1, 105–108, Jan. 1991.

4. Guo, Y. and H. Uberall, "Bistatic radar scattering by a chaff cloud," *IEEE Transaction on Antennas and Propagation*, Vol. 40, No. 7, 837–841, Jul. 1992.
5. Zhang, M., Z. S. Wu, and K. X. Liu, "Monte Carlo simulations of the EM bistatic scattering from a novel foil cloud," *5th International Symposium on Antennas, Propagation and EM Theory*, 45–49, Beijing, China, Aug. 15–18, 2000.
6. Wang, X. S., Z. J. Chen, and Y. Z. Li, "Polarization scattering characteristics of chaff cloud in outer space," *2001 CIE International Conference on Radar*, 444–448, Beijing, China, Oct. 2001.
7. Marcus, S. W., "Electromagnetic wave propagation through chaff clouds," *IEEE Transaction on Antennas and Propagation*, Vol. 55, 2032–2042, Jul. 2007.
8. Marcus, S. W., "Incoherent scattering from dense clouds of wire dipoles," *IEEE Antennas and Propagation Society International Symposium*, 1–4, San Diego, USA, Jul. 5–11, 2008.
9. Illahi, A., M. Afzaal, and Q. A. Naqvi, "Scattering of dipole field by a perfect electromagnetic conductor cylinder," *Progress In Electromagnetics Research Letters*, Vol. 4, 43–53, 2008.
10. Hatamzadeh-Varmazyar, S. and M. Naser-Moghadasi, "New numerical method for determining the scattered electromagnetic fields from thin wires," *Progress In Electromagnetics Research B*, Vol. 3, 207–218, 2008.
11. Palermo, C. J. and L. H. Bauer, "Bistatic scattering cross section of chaff dipoles with application to communications," *Proceedings of the IEEE*, Vol. 53, 1119–1121, Aug. 1965.
12. Arnott, W. P., A. Huggins, J. Gilles, D. Kingsmill, and J. Walker, "Determination of radar decoy diameter distribution function, fall speed, and concentration in the atmosphere by use of the NEXRAD radar," Desert Research Institute, Reno, USA, 2004, Available: http://www.patarnott.com/pdf/decoyRadarandFallSpeed.pdf.
13. Jenn, D. C., *Radar and Laser Cross Section Engineering*, 2nd Edition, Ch. 3, 2005.
14. Ishimaru, A., *Wave Propagation and Scattering in Random Media*, Wiely-IEEE Press, 1994.